Spontaneous Breakdown of Topological Protection in Two Dimensions

Jianhui Wang,[1] Yigal Meir,[1,2] and Yuval Gefen[3]
[1]Department of Physics, Ben-Gurion University of the Negev, Beer Sheva 84105, Israel
[2]Ilse Katz Institute for Nanoscale Science and Technology, Ben-Gurion University of the Negev, Beer Sheva 84105, Israel
[3]Department of Condensed Matter Physics, Weizmann Institute of Science, Rehovot 76100, Israel
(Received 29 September 2016; published 26 January 2017)

Because of time-reversal symmetry, two-dimensional topological insulators support counterpropagating helical edge modes. Here we show that, unlike the infinitely sharp edge potential utilized in traditional calculations, an experimentally more realistic smooth edge potential gives rise to edge reconstruction and, consequently, spontaneous time-reversal symmetry breaking. Such edge reconstruction may lead to breaking of the expected perfect conductance quantization, to a finite Hall resistance at zero magnetic field, and to a spin current. This calculation underpins the fragility of the topological protection in realistic systems, which is of crucial importance in proposed applications.

DOI: 10.1103/PhysRevLett.118.046801

Introduction.—The quantum spin-Hall phase, a class of topological phase, was originally proposed for graphene [1], and has been subsequently understood [2] to be more relevant for HgTe quantum wells, a prediction that was later verified experimentally [3]. This topological insulator (TI) phase supports helical edge modes, the only source of conduction in the system at low energies. In the quantum spin-Hall phase, time-reversal symmetry (TRS) is expected to guarantee no net equilibrium charge current at the edge. The time-reversed edge modes appear as pairs, implying zero quantum Hall conductance, but finite quantized spin-Hall conductance. Originally the Bernevig-Zhang (BZ) model [4], describing zinc-blende materials under shear strain, this phase was treated as a juxtaposition of two $\nu = 1$ quantum Hall liquids of opposite spins with opposite directions of magnetic field. It was later realized [2] that such a phase may emerge in materials with intrinsic spin-orbit interactions, without an external strain, captured by the Bernevig-Hughes-Zhang (BHZ) model [2]. Most importantly, these two models employed sharp boundary conditions. Here we generalize these models to the realistic case of smooth boundary conditions and demonstrate that TRS may be spontaneously broken, leading, for example, to spin current and finite Hall conductance at zero magnetic field. Importantly, this undermines the topological protection against backscattering at the edge. Moreover, we predict that the two terminal conductance through a quantum point contact will exhibit a conductance step at $1 \times e^2/h$, in addition to the expected plateau at $2e^2/h$.

The physics of this phenomenon is rather straightforward. Assume that the density of electrons is determined by an external gate. Then, in order to minimize the dominant Coulomb energy, the electron density tries to mimic the positive-charge distribution on the gate. If the latter falls smoothly to zero near the edge of the system, the electron density can try to follow suit by separation of the edge modes, each giving rise to a decrease in density. The smoother the confining potential, the larger the separation between the edge modes. This observation is a natural generalization of the edge-reconstruction scenario predicted [5–11] and observed [12–15] in the quantum Hall regime, only that in the present case the edge modes are of opposite chiralities, which leads to spontaneous breaking of TRS. Below, we demonstrate the emergence of this phenomenon based on a microscopic analysis of the two models mentioned above.

BZ model.—In this model [4] the strain induced spin-orbital coupling is incorporated into the continuum limit of the conduction band, leading, for appropriate strain configurations, to an effective magnetic field in either the symmetric gauge or the Landau gauge. Hence, the spectrum consists simply of the familiar Landau levels. However, in contrast to the case of an actual external magnetic field, the direction of the effective magnetic field is opposite for the two spin species. Hence, setting the chemical potential such that only the lowest Landau level is occupied results in a pair of counterpropagating edge modes, one for each spin species. Since the two edge modes are related by time-reversal transformation, elastic single-particle backscattering is forbidden unless there is explicit breaking of TRS due to, e.g., magnetic impurities. Even though other backscattering processes such as inelastic single-particle backscattering, two-particle backscattering, and interaction induced scattering are allowed [16–20], these processes are irrelevant in the renormalization-group sense unless the density-density interaction between the two edge modes is sufficiently strong.

The above studies did not take into account the interplay between the confining potential and electron-electron interactions. This was addressed in the context of both the integer [5,6,21] and the fractional [7,8] quantum Hall regimes. For the specific case of filling factor $\nu = 1$, it was found [6],

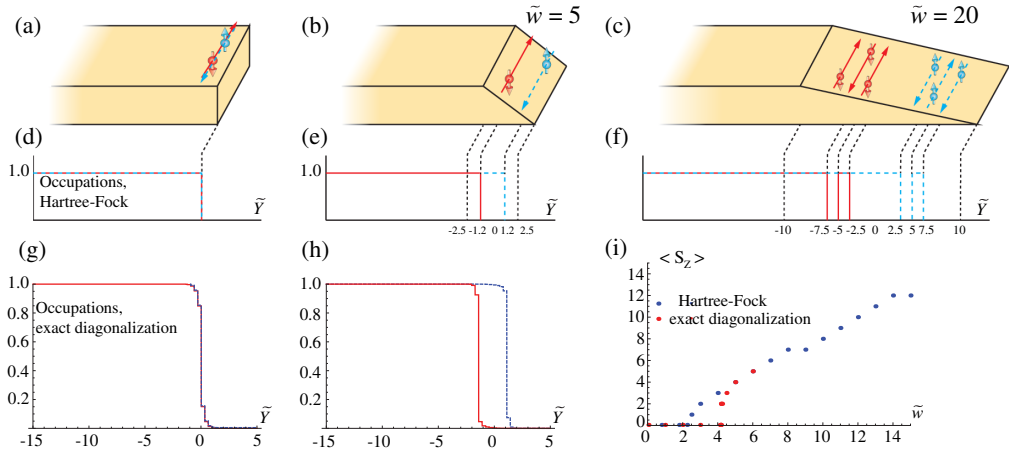

FIG. 1. Edge reconstruction for the BZ model. Panels (a)–(c) describe the schematics of the results for three different distributions of the confining positive charge (light orange), characterized by $\tilde{w}$, the length scale over which it decays to zero. The edge modes are marked by broken blue (spin up) and solid red (spin down) lines. Panels (d)–(f) depict the occupations of the electronic states, using the Hartree-Fock approximation, demonstrating a single drop in density for a sharp edge ($\tilde{w} = 0$) in (d), spin separation for smoother edge ($\tilde{w} = 5$) in (e), and Chamon-Wen-like reconstruction in (f) for an even smoother edge ($\tilde{w} = 20$). $\tilde{Y}$ denotes the position of state, in units of ℓ (the effective magnetic length); $\tilde{Y} = 0$ is the center of the density drop. Panels (g) and (h) depict the same distributions as in (d) and (f), respectively, using exact diagonalization. Panel (i) depicts the edge spin magnetization as a function of the slope of the positive-charge density, suggesting a continuous phase transition.

employing the Hartree-Fock (HF) approximation, that when the confining potential is smooth enough, some electrons would detach themselves from the bulk and form an additional $\nu = 1$ strip several magnetic lengths away from the main bulk of electron density. In other words, the occupation number as a function of the guiding center coordinate (i.e., the center of the single-particle wave function in the Landau gauge) goes down from 1 to 0, then again back to 1, then it goes down to 0 and remains at 0, as one moves from the interior of the electron liquid to the exterior [cf. the red or blue curve in Fig. 1(f)]. Accordingly, there is now an additional pair of counterpropagating edge modes on the outer side of the original one. This picture has been qualitatively confirmed by exact diagonalization calculations [6]. Similar physics arises, for example, at the $\nu = 2/3$ fractional quantum Hall regime [7,8], where an additional $\nu = 1/3$ strip forms outside the minimum edge structure required by the bulk topological order [22]. This latter picture was recently used by us [23] to provide a unified framework for the major experimental results in the $\nu = 2/3$ fractional quantum Hall regime [24–26], and is also supported by other recent experimental works [14,27,28]. Considering the similarity between quantum Hall states and the BZ model, it is natural to ask whether a related edge reconstruction takes place within the BZ picture, too.

To check this similitude, we have studied the BZ model in the presence of a uniform positive background charge density that decays linearly to zero at the edge of the system [Figs 1(a)–1(c)] over a length scale $\tilde{w}$ (measured in units of the magnetic length $\sqrt{\hbar c/eB}$, where $\hbar$ is the Planck constant, c is the velocity of light, e is the electron charge, and B is the effective magnetic field, determined in the BZ model by the applied strain). We first employed a HF approximation [29], which gave rise to three different regimes. When $\tilde{w}$ is small, we find a compact spin-unpolarized ground state [Fig. 1(d)]: as one approaches the edge, the occupation of each of the effective Landau levels drops from 1 to 0 at the same point (the HF analysis only allows filled or empty single-particle states). This is the standard picture, compatible with calculations employing a sharp edge. As $\tilde{w}$ increases (smaller slope of the positive background charge), spin polarization forms [Fig. 1(e)], marking the onset of a zero temperature (continuous) phase transition. Similarly to the quantum Hall setup, as the gradient of the positive-charge background is made smaller, a single sharp drop in the electron density (as one moves towards the edge) would create a dipolelike charge distribution [6]. To reduce the electronic energy, a more moderate decrease of the electron density is required. In this regime ($\tilde{w} > \tilde{w}_{c1}$, where $\tilde{w}_{c1} \approx 2.3$–$2.4$), the energy minimizing configuration consists of two consecutive steps of the electron density, at two different distances from the edge, leading to the formation of a spin-polarized strip near the edge. As $\tilde{w}$ is further increased, the width of this strip and, as a consequence, the total spin polarization S_z, increases [Fig. 1(i)]. Once the value of $\tilde{w}$ is sufficiently large ($\tilde{w} > \tilde{w}_{c2}$, where $\tilde{w}_{c2} \approx 19$–$20$), the screening of the background charge by two separate steps of the respective spin-polarized density profiles becomes poor, leading eventually to a Chamon-Wen-type reconstruction [6] within each spin species [Fig. 1(f)]. The occupation numbers and real space electronic density for each spin species are now nonmonotonic, representing the emergence of additional strips within each spin species.

To corroborate the predictions of the HF analysis, we have also performed exact diagonalization calculations for the lower range of values of $\tilde{w}$ [29]. For small values of $\tilde{w}$, we have found again an unpolarized ground state [Fig. 1(g)]. As $\tilde{w}$ is increased, the occupancy becomes smoother, until, at larger $\tilde{w}$, we find again the emergence of spontaneous polarization [Fig. 1(h)]. The value of S_z agrees with the HF prediction (for a given $\tilde{w}$), even though the critical $\tilde{w}_{c1} \approx 4.18$ is slightly larger. To summarize, the Hartree-Fock approximation captures the essence of the problem.

Experimental consequences.—The spontaneous polarization found above has important experimental implications. Since polarization means that TRS is spontaneously broken, elastic single-particle backscattering is no longer forbidden. It is well known that such a process is relevant in the renormalization-group sense for repulsive density-density electron interaction (owing to the spatial separation of the two edge modes in the spin-polarized phase, the bare backscattering amplitude should not be large). We thus expect that the violation of conductance quantization originating from edge transport will be observed as temperature is decreased, or the sample length increases. One may thus explore the spontaneous breaking of TRS by measuring edge transport in that regime. Only at lower temperatures is localization expected to eventually take place [16,18]. This result may resolve the hitherto unexplained puzzle that transport in two-dimensional TIs appears to be ballistic as long as the samples are small [3,32], but longer samples (longer edges) exhibit lower conductance [3,33,34], providing evidence for backscattering.

An even starker demonstration of TRS breaking is provided by the setup depicted in Fig. 2(a), consisting of a standard quantum point contact (QPC) positioned in the middle of a six-terminal device. For example, tuning the voltage on the split gate so that the inner edge mode is completely reflected and the outer edge mode is still fully transmitted, the longitudinal and Hall resistance as functions of the split-gate voltage should have plateaus at $R_{xx} = (2h/3e^2)$ and $R_{xy} = (h/3e^2)$, respectively (for the derivation, see Ref. [29]). In the general case, where the transmission probability of the outer (inner) channel is T_O (T_I), $R_{xx} = (3 - T_O - T_I)/(3T_I + 3T_O - 4T_I T_O)h/e^2$ and $R_{xy} = (T_O - T_I)/(3T_I + 3T_O - 4T_I T_O)h/e^2$ (the sign of R_{xy} depends on the way TRS is spontaneously broken). The two-terminal conductance, given by $G_{\text{2-terminal}} = (T_O + T_I)e^2/h$, exhibits conductance steps at $2 \times e^2/h$, $1 \times e^2/h, 0$. Similar steps in the conductance were observed in the quantum Hall effects [24,25], and were regarded as evidence for edge reconstruction [23,35]. We thus predict a finite Hall resistance at zero magnetic field due to the spontaneous breaking of TRS. Another important consequence of the breaking of TRS is the possible generation of spin current. Since the spin is a good quantum number in each of the edge modes, reflection of one edge mode necessarily means that only one spin direction is transmitted. The transmitted edge mode can be utilized at another point in the device as a source for a specific spin. As mentioned above, in the absence of external TRS breaking, there is equal probability for the spin current to be in either direction. To tune the spin current in a specific direction, a weak external magnetic field in the desired spin direction may be applied.

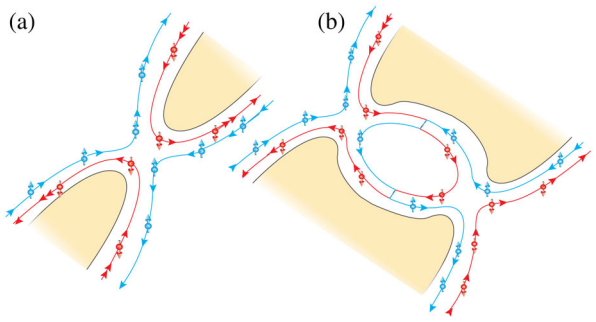

FIG. 2. Experimental devices for detecting spontaneous spin polarization. The electron's gas is depleted in the yellow regions. Only a small part of the sample under the split gates is shown. (a) A quantum point contact may be tuned to reflect one spin channel and transmit the other, resulting in a quantum Hall effect at zero magnetic field, and spin current. (b) If the spin polarization happens to be opposite on the two sides of the two-point contact setup, a situation where each one transmits one channel but the total transmission is zero may arise.

Since there is *a priori* full symmetry between the two edge modes, the following intriguing situation may arise when two such QPCs are put in series. Assume that the spontaneous symmetry breaking is different on the two sides of the sample [left and right in Fig. 2(b)]. Thus, the two edge channels have to cross each other, on the top and bottom edges of the sample. Such a crossing defines a domain wall between a spin-up and a spin-down region. As it costs exchange energy, it will probably happen at the most once for each edge at low temperatures. Thus, if this crossing occurs somewhere between the two QPCs, the conductance through each QPC is finite ($= 1 \times e^2/h$), while the conductance through the two QPCs in series vanishes.

BHZ model.—The BZ model was originally developed to predict and describe topologically insulating behavior in zinc-blende semiconductors such as GaAs. Presently, however, the experimentally most studied two-dimensional TI is the mercury telluride (HgTe) quantum well, which is more faithfully described by the BHZ model [2]. This model employs the relevant band structure that leads to band inversion [36] at specific well thickness, and nontrivial topological order. In order to check the relevance of the physical picture described above to the BHZ model, we have performed HF calculations for this model in the presence of a linear confining potential at the edge [29]. As with the BZ model, and as found in previous studies, when the confining potential is steep (i.e., the single-particle wave function vanishes at the edge but there is no other external potential),

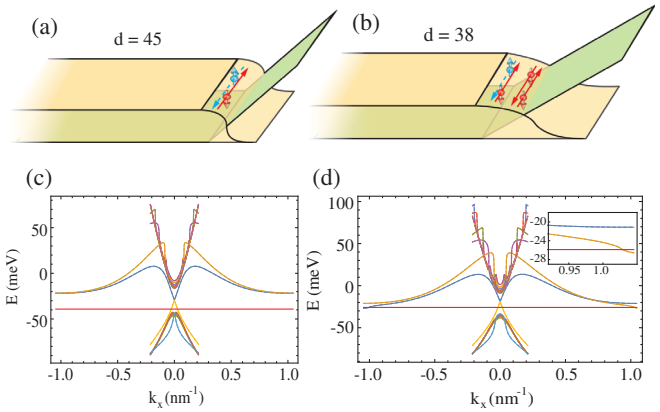

FIG. 3. Edge reconstruction in the Bernevig-Hughes-Zhang model. (a),(b) Schematic presentation of the reconstruction as a function of the slope of the linear confining potential. For a sharp potential (a) each edge supports a single pair of edge modes of opposite spin and opposite direction. For a smoother edge (b) an additional pair of same-spin, counterpropagating edge states emerges near the edge. Panels (c) and (d) depict the spectra for these two cases, where for the sharp potential the chemical potential intersects the spectrum at two energies, while for the smoother potential, two additional crossings give rise to two additional edge modes.

there is no spin polarization or edge reconstruction [Fig. 3(a)]—there is a single pair of counterpropagating, opposite-spin edge modes. Figure 3(c) shows the corresponding spectrum: the chemical potential intersects the spectrum for each spin at two points, leading to two edge modes on the two edges of the system. However, as the confining potential becomes shallower (13 meV/nm for the set of parameters used in our simulations, taken from Ref. [30]) we observe edge reconstruction [Fig. 3(b)]—a new pair of counterpropagating edge modes emerges near the edge. Interestingly, unlike the original counterpropagating edge modes, which are of opposite spins, the reconstructed counterpropagating ones are of the same spin. The emergence of a pair of counterpropagating same-spin edge modes is very similar to the Chamon-Wen reconstruction [6]. The fact that the lowest energy state displays edge reconstruction only in one of the spin channels is due to the gain in exchange energy. The corresponding spectrum for this spin species [Fig. 3(d)] shows two additional crossings of the chemical potential with the spectrum. Thus, as with the BZ model, a smoother edge leads to spontaneous breaking of TRS. This symmetry breaking facilitates backscattering between counterpropagating opposite-spin edge state, leading to increase in the resistance. Moreover, the resulting difference in spin-density profiles near the edge leads to different tunneling amplitudes of the two spin directions at a quantum point contact. This yields, again in agreement with the results of the BZ model, (i) a finite spin current and a finite Hall conductance at zero magnetic field, as well as (ii) possible transmission blockade through two QPCs in series [Fig. 2(b)].

Discussion.—The analysis presented here shows that a realistic smooth edge potential may lead to spontaneous breaking of TRS as well as to the appearance of additional edge modes in two-dimensional topological insulators. The broken TRS undermines topological protection and gives rise to a finite backscattering length scale ℓ_{BS}. For relatively short samples, of length $L \lesssim \ell_{\mathrm{BS}}$, the resistance will be quantized. Introducing a QPC leads to a quantized Hall resistance at zero magnetic field (one mode is perfectly reflected, while the other is perfectly transmitted [Fig. 2(a) and Eqs. (1) and (2)]. This is accompanied by quantized steps of the two-terminal conductance, as the QPC is pinched off. Moreover, an intricate transmission blockade through two QPCs in series may arise [Fig. 2(b). For longer systems $L > \ell_{\mathrm{BS}}$, backscattering results in deviations from conductance quantization, possibly in line with the observation of a higher resistance in HgTe quantum wells [3,33,34]. On even longer length scales, $L \gg \ell_{\mathrm{BS}}$, backscattering may lead to Anderson localization at the edge. These intriguing predictions, including the emergence of net spin current at zero magnetic field, are amenable to experimental test.

The applicability of the present study goes much further than TIs. It includes the quantum spin-Hall effect in graphene, subject to strong magnetic field [37]. The fact that edge reconstruction has been predicted [7,8] and observed [14,15] also in the fractional quantum Hall regime suggests extensions to fractional TIs [38,39]. It would be intriguing to explore the additional effects due to the fractional charge of the reconstructed edge state, and whether, e.g., one can also generate, in this case, neutral edge modes in TIs [26,40]. The present study may also put severe constraints on possible utilization of TIs, from spintronics to quantum computation [41]. As demonstrated here, a smooth edge is detrimental to topological protection. For example, employing the appropriate parameters for HgTe [30], we find that at the edge-reconstruction transition, the bulk electron density drops to zero at the edge on a scale of 10 nm. The scale determined by the distance to the electrical gates is typically much larger, implying that we are always in the edge-reconstructed regime, unless special care is taken in defining the edge or the contacts of the device.

J. W. acknowledges support provided by the Kreitman Foundation. Y. M. acknowledges ISF Grant No. 292/15. Y. G. acknowledges support from ISF Grant No. 1349/14, DFG Grant No. RO 2247/8-1, CRC 183 of the DFG, the IMOS Israel-Russia program, and Minerva. Y. G. acknowledges discussions with I. Burmistrov, I. Gornyi, and A. Mirlin.

[1] C. L. Kane and E. J. Mele, Phys. Rev. Lett. **95**, 226801 (2005).
[2] B. A. Bernevig, T. L. Hughes, and S.-C. Zhang, Science **314**, 1757 (2006).

[3] M. König, S. Wiedmann, C. Brüne, A. Roth, H. Buhmann, L. W. Molenkamp, X.-L. Qi, and S.-C. Zhang, Science **318**, 766 (2007).
[4] B. A. Bernevig and S.-C. Zhang, Phys. Rev. Lett. **96**, 106802 (2006).
[5] J. Dempsey, B. Y. Gelfand, and B. I. Halperin, Phys. Rev. Lett. **70**, 3639 (1993).
[6] C. de C. Chamon and X. G. Wen, Phys. Rev. B **49**, 8227 (1994).
[7] Y. Meir, Phys. Rev. Lett. **72**, 2624 (1994).
[8] Y. Meir, Int. J. Mod. Phys. B **10**, 1425 (1996).
[9] X. Wan, K. Yang, and E. H. Rezayi, Phys. Rev. Lett. **88**, 056802 (2002).
[10] K. Yang, Phys. Rev. Lett. **91**, 036802 (2003).
[11] Y. Barlas, Y. N. Joglekar, and K. Yang, Phys. Rev. B **83**, 205307 (2011).
[12] O. Klein, C. de C. Chamon, D. Tang, D. M. Abusch-Magder, U. Meirav, X. G. Wen, M. A. Kastner, and S. J. Wind, Phys. Rev. Lett. **74**, 785 (1995).
[13] N. B. Zhitenev, M. Brodsky, R. C. Ashoori, and M. R. Melloch, Phys. Rev. Lett. **77**, 1833 (1996).
[14] V. Venkatachalam, S. Hart, L. Pfeiffer, K. West, and A. Yacoby, Nat. Phys. **8**, 676 (2012).
[15] A. Grivnin, H. Inoue, Y. Ronen, Y. Baum, M. Heiblum, V. Umansky, and D. Mahalu, Phys. Rev. Lett. **113**, 266803 (2014).
[16] C. Wu, B. A. Bernevig, and S.-C. Zhang, Phys. Rev. Lett. **96**, 106401 (2006).
[17] C. Xu and J. E. Moore, Phys. Rev. B **73**, 045322 (2006).
[18] N. Lezmy, Y. Oreg, and M. Berkooz, Phys. Rev. B **85**, 235304 (2012).
[19] J. I. Väyrynen, M. Goldstein, and L. I. Glazman, Phys. Rev. Lett. **110**, 216402 (2013).
[20] J. I. Väyrynen, M. Goldstein, Y. Gefen, and L. I. Glazman, Phys. Rev. B **90**, 115309 (2014).
[21] D. B. Chklovskii, B. I. Shklovskii, and L. I. Glazman, Phys. Rev. B **46**, 4026 (1992).
[22] X.-G. Wen, Adv. Phys. **44**, 405 (1995).
[23] J. Wang, Y. Meir, and Y. Gefen, Phys. Rev. Lett. **111**, 246803 (2013).
[24] A. M. Chang and J. E. Cunningham, Phys. Rev. Lett. **69**, 2114 (1992).
[25] A. Bid, N. Ofek, M. Heiblum, V. Umansky, and D. Mahalu, Phys. Rev. Lett. **103**, 236802 (2009).
[26] A. Bid, N. Ofek, H. Inoue, M. Heiblum, C. L. Kane, V. Umansky, and D. Mahalu, Nature (London) **466**, 585 (2010).
[27] N. Paradiso, S. Heun, S. Roddaro, L. Sorba, F. Beltram, G. Biasiol, L. N. Pfeiffer, and K. W. West, Phys. Rev. Lett. **108**, 246801 (2012).
[28] R. Sabo, I. Gurman, A. Rosenblatt, F. Lafont, D. Banitt, J. Park, M. Heiblum, Y. Gefen, V. Umansky, and D. Mahalu, arXiv:1603.06909.
[29] See Supplemental Material at http://link.aps.org/supplemental/10.1103/PhysRevLett.118.046801 for details of the calculations of the ground state structures and transport coefficients and more discussion of the reconstructed edge structures for the BHZ model, which includes Refs. [6,30,31].
[30] M. König, H. Buhmann, L. W. Molenkamp, T. Hughes, C.-X. Liu, X.-L. Qi, and S.-C. Zhang, J. Phys. Soc. Jpn. **77**, 031007 (2008).
[31] M. Büttiker, Phys. Rev. B **38**, 9375 (1988).
[32] A. Roth, C. Brüne, H. Buhmann, L. W. Molenkamp, J. Maciejko, X.-L. Qi, and S.-C. Zhang, Science **325**, 294 (2009).
[33] I. Knez, R.-R. Du, and G. Sullivan, Phys. Rev. Lett. **107**, 136603 (2011).
[34] I. Knez, C. T. Rettner, S.-H. Yang, S. S. P. Parkin, L. Du, R.-R. Du, and G. Sullivan, Phys. Rev. Lett. **112**, 026602 (2014).
[35] C. W. J. Beenakker, Phys. Rev. Lett. **64**, 216 (1990).
[36] B. A. Volkov and O. A. Pankratov, Piz'ma Zh. Exp. Teor. Fiz. **42**, 145 (1985) [JETP Lett. **42**, 178 (1985)].
[37] A. F. Young, J. D. Sanchez-Yamagishi, B. Hunt, S. H. Choi, K. Watanabe, T. Taniguchi, R. C. Ashoori, and P. Jarillo-Herrero, Nature (London) **505**, 528 (2014).
[38] M. Levin and A. Stern, Phys. Rev. Lett. **103**, 196803 (2009).
[39] M. Levin and A. Stern, Phys. Rev. B **86**, 115131 (2012).
[40] C. L. Kane, M. P. A. Fisher, and J. Polchinski, Phys. Rev. Lett. **72**, 4129 (1994).
[41] M. Z. Hasan and C. L. Kane, Rev. Mod. Phys. **82**, 3045 (2010).